

# Dissociation of brain areas associated with force production and stabilization during manipulation of unstable objects

Linda Holmström · Örjan de Manzano · Brigitte Vollmer ·  
Lea Forsman · Francisco J. Valero-Cuevas · Fredrik Ullén ·  
Hans Forssberg

Received: 23 May 2011 / Accepted: 2 October 2011 / Published online: 25 October 2011  
© Springer-Verlag 2011

**Abstract** Multifinger dexterous manipulation of unstable or deformable objects requires control of both direction and magnitude of fingertip force vectors. Our aim was to study the neuroanatomical correlates of these two distinct control functions. Brain activity was measured using functional magnetic resonance imaging while 16 male subjects (age: 26–42,  $M = 32$ ,  $SD \pm 4$  years) compressed four springs representing a  $2 \times 2$  factorial design with two levels of force and instability requirements. Significant activations associated with higher instability were located bilaterally in the precentral gyri, the postcentral gyrus, and the cerebellum. In the main effect for high force, activity was found in areas located in the primary motor regions contralateral to the active hand and bilaterally in the cerebellum. An overlap in activation between the two main effects was found bilaterally in the cerebellum (lobule VI). This study not only confirms a recently described bilateral fronto-parieto-cerebellar network for manipulation of increasingly unstable objects, but critically extends our understanding by describing its differentiated modulation with both force

magnitude and instability requirements. Our results, therefore, expose a previously unrecognized and context-sensitive system of brain regions that enable dexterous manipulation for different force magnitude and instability requirements of the task.

**Keywords** Unstable object manipulation · Precision grip · Grasping network · Motor cortex · Cerebellum

## Introduction

Precise control of fingertip forces is critical for dexterous manipulation. More specifically, both the magnitude and direction of forces have to be controlled at the contact surface of the object to achieve task goals. In daily life, we often handle unstable or deformable objects. Such manipulation stresses the demands on dynamic on-line adjustments of both direction and magnitude of fingertip forces. In seminal studies, Johansson et al. have shown that internal representations of object properties are stored and used to program force output in advance and that sensory information is used to adjust the fingertip forces on-line, as well as to update the internal representation of the object (Johansson and Flanagan 2009). To study this dynamic control of force, Valero-Cuevas et al. (2003) developed the strength–dexterity paradigm, in which helical springs are compressed without allowing the spring to buckle. The stiffness and slenderness of the spring sets the requirement of fingertip force magnitude and direction, respectively. Recently, we reported a gradual development in ability to compress more difficult springs (increasing force and instability requirements) in typically developing children (Vollmer et al. 2010). Performance co-varied with grip strength and gross manual dexterity, but also showed a

---

L. Holmström (✉) · Ö. de Manzano · B. Vollmer ·  
L. Forsman · F. Ullén · H. Forssberg  
Neuropediatric Research Unit,  
Department of Women's and Children's Health,  
Karolinska Institutet, Astrid Lindgren Children's Hospital  
Q2:O7, 171 76 Stockholm, Sweden  
e-mail: linda.holmstrom@ki.se

L. Holmström · Ö. de Manzano · B. Vollmer · L. Forsman ·  
F. Ullén · H. Forssberg  
Stockholm Brain Institute, Stockholm, Sweden

F. J. Valero-Cuevas  
Division of Biokinesiology and Physical Therapy, Department of  
Biomedical Engineering, University of Southern California,  
Los Angeles, CA, USA

unique latent trait, indicating individual differences in dynamic sensorimotor control of fingertip force direction.

The neural network involved in precision grip and object manipulation has been explored in several fMRI studies (Binkofski et al. 1999a; Ehrsson et al. 2001, 2002; Kuitzbuschbeck et al. 2001). It consists of a bilateral frontoparieto-cerebellar network, that is, primary sensorimotor cortex (M1/S1), dorsal and ventral premotor cortices (PMD and PMV), supplementary and cingulate motor areas (SMA and CMA), and the cortex lining the intraparietal sulcus and the cerebellum. Parts of this network are involved in the control of the force magnitude, although the relation between employed force magnitude and brain activity is complex. Both positive (contralateral M1/S1, SMA/CMA and ipsilateral cerebellum) and negative correlations (bilateral PMV, anterior portions of SMA/CMA, and ipsilateral posterior parietal regions) have been reported (Kuitzbuschbeck et al. 2008). A recent TMS study suggested that PMV is involved in the predictive control of fingertip forces (Dafotakis et al. 2008). Less is known about brain areas involved in the control of fingertip force direction. Recent fMRI studies report varying brain activity depending on the complexity of the unstable object (Milner et al. 2007; Mosier et al. 2011; Talati et al. 2005). It is, however, unclear to what extent control of finger force direction and force magnitude overlap in terms of regions involved within this network.

In this study, we investigate brain activity during object manipulation when both the force magnitude and instability requirements for manipulation are varied in the same type of object. We use fMRI to measure brain activity during compression of four springs with different mechanical properties, representing a  $2 \times 2$  factorial design with two levels of force and instability requirements.

## Materials and methods

### Participants

A convenience sample of 19 right-handed men with no reported history of neurological disease participated in the study. The participants were given full information regarding the nature and conduct of the experiment at the time of recruitment. Imaging data from one participant were excluded because of a technical failure with the MR scanner, and data from another two participants who failed to perform according to instructions were also discarded. Hence, 16 participants (age: 26–42,  $M = 32$ ,  $SD \pm 4$  years) were included in the final analysis. The experimental procedures were undertaken with the understanding and written consent of each participant and were ethically approved by the Regional Ethical Committee, Stockholm, Sweden.

### Behavioral paradigm

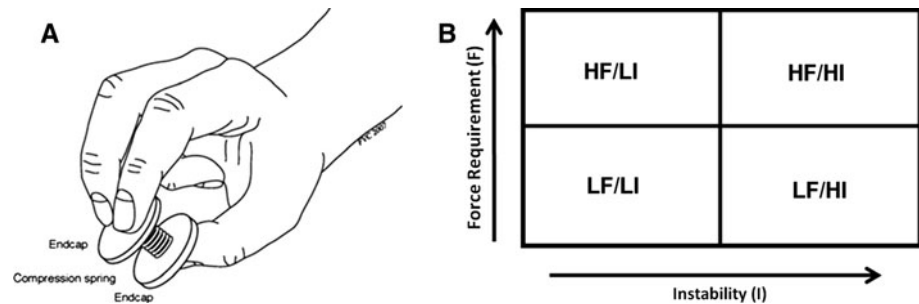
Subjects were instructed to compress each spring while preventing them from buckling. Depending on the geometry and material properties of the spring, this task requires the control of both direction and magnitude of fingertip forces based on sensory feedback (Valero-Cuevas et al. 2003). Briefly, the strength–dexterity (S-D) paradigm quantifies the dynamic interaction between fingertip force magnitude (strength) and directional control (dexterity) during pinch (Valero-Cuevas et al. 2003; Talati et al. 2005; Vollmer et al. 2010; Mosier et al. 2011). The S-D test is based on the principle of buckling of compression springs, with different strength and dexterity requirements. The strength requirement is defined as the pinch force necessary to compress the spring to solid length. The dexterity requirement is defined as the ability to compress the spring without buckling. To prevent buckling, the posture of the fingers and the direction of fingertip forces need to be dynamically regulated to stabilize the spring during compression. Four MR-compatible metal springs were constructed to correspond to two levels (high–low) of (1) force magnitude (strength of normal force) to compress the spring to its solid length and (2) instability index, that is, range of the stability limits within which the direction of the force vector has to be controlled. This was achieved by varying the number of coils, the thickness of the thread, and the diameter of the spring, respectively. Each spring had two plastic end caps large enough to allow for an opposing two finger-thumb precision grip (see Fig. 1a). The plastic end caps were covered with a thin rubber sheet to increase friction and decrease slippage. The four springs covered four distinct strength–dexterity combinations: HF/LI (high force/low instability), LF/LI (low force/low instability), HF/HI (high force/high instability), and LF/HI (low force/high instability). Specifically, any dependence of the force versus stability features should be eclipsed by the fact that the four springs impose tasks for which the force and stability features are distinct.

### Design and procedure

The experiment was designed as a  $2 \times 2$  factorial design (Fig. 1b), with the four springs constituting two levels of the two factors “force magnitude” and “instability”. This design allows for investigating main effects, non-additive synergistic interactions as well as overlap in terms of brain activity between the two factors. A “rest” condition was also included as part of the implicit baseline.

All experiments were conducted at the MR center of the Karolinska University Hospital in Stockholm, Sweden. Upon arrival, the participants were informed again about the purpose of the study, experimental paradigm and MR

**Fig. 1 a, b** Compression springs and design. **a** Compression spring and correct finger position. **b**  $2 \times 2$  factorial design, HF/LI (high force/low instability), LF/LI (low force/low instability), HF/HI (high force/high instability), LF/HI (low force/high instability)



safety procedures. Detailed instructions were then given about the experimental procedures, during which the participant could try out the different springs. This instruction/preparation period lasted for approximately 10 min.

A pillow was placed under the participants' right arm to support it and minimize muscle activity not directly required for compressing the springs. The participants were told to move only the fingers during the active conditions and refrain from movement during the rest condition. Earplugs were provided to block scanner noise. In addition, headphones further reduced noise and allowed for verbal instructions. Each scanning session was composed of twenty-five epochs corresponding to five presentations of each condition. Each participant performed two scanning sessions. An epoch of the experiment consisted of two parts—Instruction and Condition—composed as follows: *Instruction*: verbal instruction, 6 s; two metronome beats (to pace the participant), 4 s (10 s cumulative); *Condition*: rest/active, ten metronome beats (corresponding to ten compressions of the spring), 20 s (30 s cumulative).

During the scanning sessions, an experimenter would stand next to the participant and exchange springs according to a pre-specified task order. The task order was constructed using permutations of the five conditions: HF/LI (high force/low instability), LF/LI (low force/low instability), HF/HI (high force/high instability), LF/HI (low force/high instability), and rest. Three constraints were imposed: (1) that neither two high force magnitude nor two high instability conditions would follow one another; (2) that all springs were presented an equal number of times; (3) that rest conditions were at most five conditions apart. These constraints were introduced to reduce the likelihood for participant fatigue. The task order was identical for all participants.

Throughout the session, instructions to the experimenter were projected onto a screen with the help of a computer-projector setup and an E-prime script (Psychological Software Tools, Inc.): (1) the next-spring-to-be-presented and (2) a countdown until the next stimulus presentation or rest. E-prime was also used to present the participant with the verbal instructions and the metronome. Participants were instructed to perform smooth cyclic compressions in synchrony with the metronome during the active

conditions. Two different instructions were given, corresponding to either the rest or active conditions: “Rest”; “You will now be given a new spring. Compress the spring in beat with the metronome.”

The experimenter responsible for exchanging the springs also monitored the participant's behavior and logged any performance errors. All participants included in the final analysis completed all conditions successfully.

#### fMRI data acquisition

Imaging was performed using a 1.5 T scanner (Signa Excite, GE Medical Systems, Milwaukee, WI, USA) with a standard eight-channel head coil. At the beginning of each scanning session, a high-resolution, three-dimensional spoiled gradient-echo T1-weighted anatomical image volume of the whole brain (voxel size  $1 \times 1 \times 1 \text{ mm}^3$ ) was collected. Functional image data were then collected using a gradient-echo, echo-planar (EPI) T2\*-weighted sequence with blood oxygenation level-dependent (BOLD) contrasts (Kwong et al. 1992; Ogawa et al. 1992), using the following parameters: echo time (TE) = 40 ms; field of view (FOV) = 22 cm; matrix size =  $64 \times 64$ ; flip angle =  $90^\circ$ ; slice thickness = 5 mm; slice spacing = 0.5 mm; repetition time (TR) = 2.5 s. Whole-brain image volumes were constructed from 32 contiguous axial slices. At the beginning of a session, four “dummy” image volumes were acquired, but not saved, to allow for equilibration effects. A total of 600 functional image volumes were obtained for each participant.

#### Data analysis

The MRI data were processed and analyzed using SPM5 (Wellcome Department of Imaging Neuroscience, London, UK).

#### Data preprocessing

All fMRI image volumes were realigned, coregistered to each individual's T1-weighted image (Ashburner and Friston 1997), segmented, normalized (Friston et al. 1995) using the template brain of the Montréal Neurological

Institute, and spatially smoothed with an isotropic Gaussian filter of 8 mm full-width-at-half-maximum.

### Statistical analysis

The fMRI data were modeled using a general linear model, where we defined four conditions of interest corresponding to the periods in each epoch when the participants compressed each of the four springs (i.e., the last 20 s of the 30 s epochs). We modeled the first 10 s of each epoch (i.e., the instruction period) as a condition of no interest. Rest was not explicitly modeled in the design matrix, but part of the implicit baseline made up of unspecified timeslots in the experiment. Movement parameters (representing six degrees of freedom) were modeled as individual regressors in the design matrix.

To illustrate the overlap in brain activity between the active conditions, we used a “minimum statistic compared to the conjunction null” analysis (Nichols et al. 2005), corresponding to a logical AND operation between the active conditions.

The following contrasts were used to examine main effects of high force magnitude and high instability, and interactions between them, respectively: (HF/LI, HF/HI)-(LF/LI, LF/HI); (HF/HI, LF/HI)-(HF/LI, LF/LI); (HF/LI, LF/HI)-(LF/LI, HF/HI) and (LF/LI, HF/HI)-(HF/LI, LF/ HI). The significance of effects was assessed using *t* statistics from every voxel in the brain to create statistical parametric maps. Analyses were first performed for contrasts of interest within participants. A second-level random effects analysis, based on summary statistics of the data from each participant, was then performed to allow inferences at group level. We report activations that were significant at  $P < 0.01$  after correction for multiple comparisons using a false discovery rate (FDR) analysis (Genovese et al. 2002), meaning that on average less than 1% of the suprathreshold voxels are false positives. An extent threshold exceeding five active voxels was used for all contrasts. Significant local peak activations were labeled according to the SPM anatomy tool box (Eickhoff et al. 2005) and verified using the human brain atlas of Duvernoy (1999) and Mayka et. al. (2006).

## Results

### Conjunction between active conditions

A conjunction analysis of the active conditions was performed to illustrate increases in activity common to all active conditions. Significant peak activations resulting from this analysis are shown in Table 1 and superimposed on a group mean normalized T1-weighted image in Fig. 2. The largest cluster of activation includes the primary and secondary

**Table 1** Peak activations for the conjunction between active conditions

Conjunction between active conditions						
Area	$P_{\text{FDR}}$	<i>T</i>	<i>Z</i>	<i>x</i>	<i>y</i>	<i>z</i>
Superior frontal gyrus (Left SMA)	<b>0.000</b>	<b>6.66</b>	<b>5.74</b>	<b>-6</b>	<b>-4</b>	<b>54</b>
Right middle frontal gyrus (PMD)	<b>0.002</b>	<b>4.24</b>	<b>3.95</b>	<b>42</b>	<b>-6</b>	<b>56</b>
Right insula	<b>0.006</b>	<b>3.90</b>	<b>3.67</b>	<b>40</b>	<b>0</b>	<b>14</b>
Left precentral gyrus (PMV)	<b>0.000</b>	<b>4.79</b>	<b>4.39</b>	<b>-58</b>	<b>4</b>	<b>32</b>
Right precentral gyrus (PMV)	<b>0.000</b>	<b>5.93</b>	<b>5.24</b>	<b>60</b>	<b>8</b>	<b>34</b>
Right precentral gyrus (PMV)	0.000	5.18	4.69	56	2	40
Left postcentral gyrus (S1)	<b>0.000</b>	<b>10.23</b>	<b>7.74</b>	<b>-42</b>	<b>-20</b>	<b>50</b>
Left postcentral gyrus (S1)	0.000	6.33	5.52	-34	-34	46
Right postcentral gyrus (S1)	<b>0.000</b>	<b>5.90</b>	<b>5.22</b>	<b>58</b>	<b>-18</b>	<b>30</b>
Right postcentral gyrus (S1)	0.000	5.87	5.20	60	-18	34
Right postcentral gyrus (S1)	0.000	5.73	5.10	64	-18	36
Right postcentral gyrus (S1)	0.003	4.19	3.91	46	-24	38
Right postcentral gyrus (S1)	0.003	4.14	3.86	42	-26	38
Left supramarginal gyrus	<b>0.000</b>	<b>8.70</b>	<b>6.97</b>	<b>-54</b>	<b>-22</b>	<b>42</b>
Left middle occipital gyrus	<b>0.000</b>	<b>5.20</b>	<b>4.71</b>	<b>-46</b>	<b>-72</b>	<b>-2</b>
Right cerebellum (VI)	<b>0.000</b>	<b>8.60</b>	<b>6.91</b>	<b>24</b>	<b>-50</b>	<b>-26</b>
Right cerebellum (IV–V)	0.000	8.10	6.63	14	-52	-22
Right cerebellum (IV–V)	0.000	7.66	6.37	8	-58	-16
Right cerebellum (IV–V)	0.000	8.03	6.59	10	-56	-18
Right cerebellum (VIII)	<b>0.000</b>	<b>5.31</b>	<b>4.79</b>	<b>20</b>	<b>-64</b>	<b>-52</b>
Cerebellar vermis	0.000	7.61	6.34	6	-62	-16

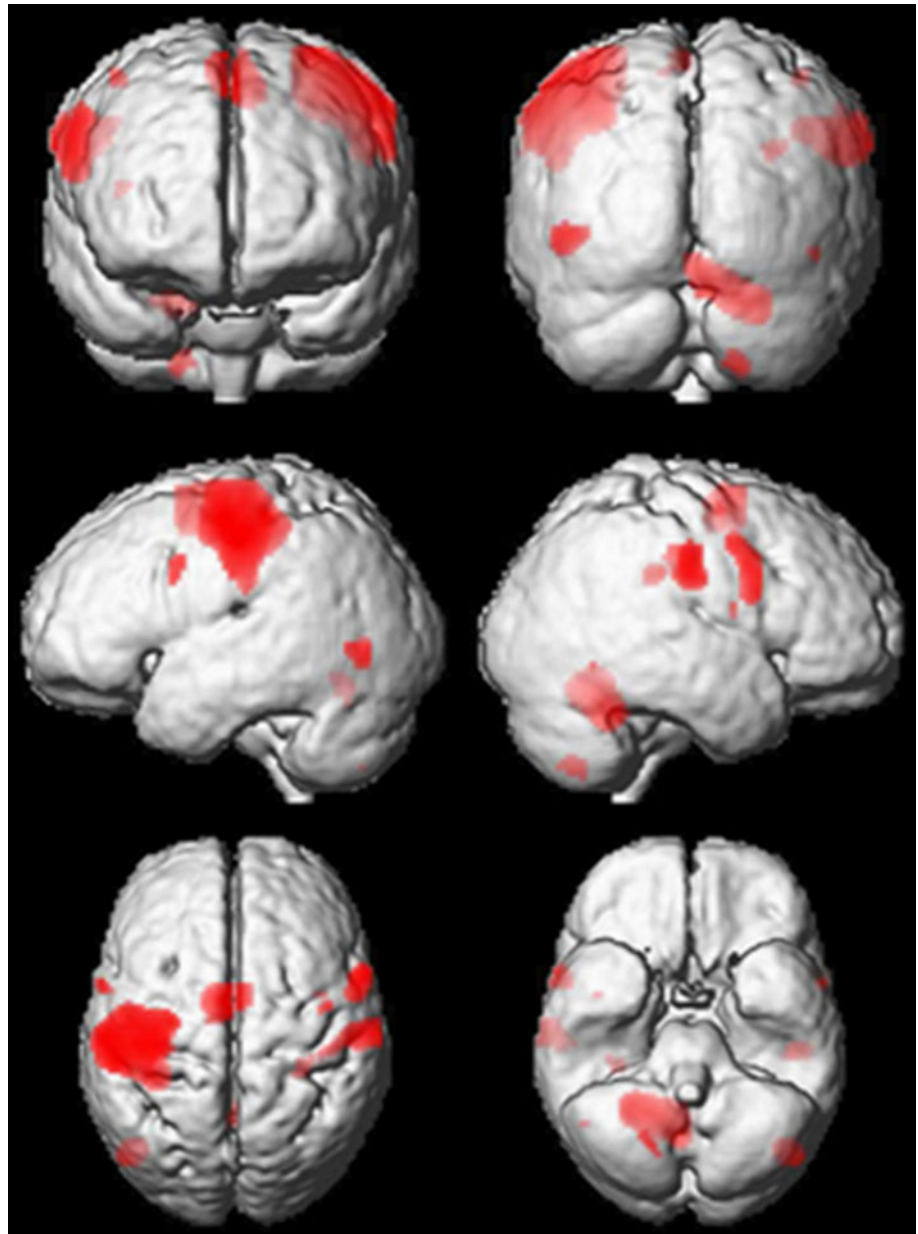
Bold font indicates main peak of activation within each cluster

sensorimotor regions contralateral (left hemisphere) to the active hand. Sensorimotor activity in the pre- and postcentral gyri was also seen in regions ipsilateral (right hemisphere) to the active hand. In addition, clusters of active voxels were seen in the supplementary motor area (SMA) and in the ipsilateral cerebellum. In the cerebellum, the largest cluster was found in the lobuli IV–V and extending into the vermis. The second largest cluster was located in the right lobule VIII.

### Factorial analysis

Based on the  $2 \times 2$  factorial design, we investigated main effects of, and interactions between, the two dimensions of

**Fig. 2** Significantly active clusters from conjunction analysis. Significantly active clusters for the conjunction between active conditions are superimposed on a three-dimensional rendering of the group mean anatomical image (T1w). Significant peak activations resulting from this analysis are found in Table 1



force and instability requirements. Results are presented in Table 2 and illustrated on a group mean normalized T1w image in Fig. 3. The histograms, in Fig. 3, show the mean adjusted BOLD response from local maxima of motor-related activations during the four different conditions, with the mean activity during rest used as baseline.

#### Regions with increased activity during compression with high instability

Significant activations associated with the main effect contrast of high instability versus low instability ([HF/HI, LF/HI]-[HF/LI, LF/LI]) are presented in Table 2 and displayed in green in Fig. 3. This contrast generated three

bilateral clusters of activation. These were located in the left and right precentral gyri, left and right postcentral gyrus/sulcus at the level of the intraparietal sulcus and left and right cerebellum, lobule VI. No “de-activations” were found when the reversed contrast ([HF/LI, LF/LI]-[HF/HI, LF/HI]) was analyzed.

#### Regions with increased activity during compression with high force magnitude

Significant activations associated with the main effect contrast of high force magnitude versus low force magnitude ([HF/LI, HF/HI]-[LF/LI, LF/HI]) are presented in Table 2 and displayed in red in Fig. 3. The high force

**Table 2** Brain activity during high versus low stability and high versus low force magnitude

High instability–low instability							High force magnitude–low force magnitude						
Area	$P_{FDR}$	$T$	$Z$	$x$	$y$	$z$	Area	$P_{FDR}$	$T$	$Z$	$x$	$y$	$z$
Left precentral gyrus (M1 <sup>a</sup> )	<b>0.004</b>	<b>6.24</b>	<b>4.32</b>	<b>-34</b>	<b>-10</b>	<b>60</b>	Left precentral gyrus (M1)	<b>0.005</b>	<b>5.74</b>	<b>4.11</b>	<b>-32</b>	<b>-26</b>	<b>58</b>
Left precentral gyrus (M1)	0.007	5.55	4.03	-30	-14	66	Left central sulcus (M1 <sup>b</sup> )	<b>0.003</b>	<b>6.32</b>	<b>4.35</b>	<b>-44</b>	<b>-20</b>	<b>52</b>
Right precentral gyrus (M1)	<b>0.004</b>	<b>6.35</b>	<b>4.36</b>	<b>36</b>	<b>-14</b>	<b>52</b>	Right medial temporal pole	<b>0.004</b>	<b>6.19</b>	<b>4.30</b>	<b>48</b>	<b>12</b>	<b>-26</b>
Left intraparietal sulcus	<b>0.003</b>	<b>6.62</b>	<b>4.46</b>	<b>-34</b>	<b>-38</b>	<b>32</b>	Right lingual gyrus	<b>0.005</b>	<b>5.74</b>	<b>4.11</b>	<b>24</b>	<b>-88</b>	<b>-6</b>
Right postcentral gyrus (S1)	<b>0.002</b>	<b>7.87</b>	<b>4.88</b>	<b>42</b>	<b>-28</b>	<b>36</b>	Right calcarine gyrus	0.006	5.24	3.89	16	-94	-2
Left cerebellum (VI)	<b>0.003</b>	<b>6.68</b>	<b>4.48</b>	<b>-18</b>	<b>-58</b>	<b>-24</b>	Left cerebellum (VIII)	<b>0.006</b>	<b>5.31</b>	<b>3.91</b>	<b>-20</b>	<b>-56</b>	<b>-40</b>
Right cerebellum (VI)	<b>0.002</b>	<b>9.17</b>	<b>5.25</b>	<b>8</b>	<b>-66</b>	<b>-20</b>	Right cerebellum (IV–V)	<b>0.002</b>	<b>9.25</b>	<b>5.27</b>	<b>10</b>	<b>-52</b>	<b>-24</b>
Right cerebellum (VI)	0.002	8.28	5.00	20	-54	-28	Right cerebellum (IX)	0.003	7.34	4.71	10	-54	-38
Right cerebellum (VI)	0.002	8.02	4.93	12	-58	-22	Right cerebellum IV–V)	0.002	8.83	5.16	16	-50	-24
							Right cerebellum (IX)	0.002	8.64	5.11	8	-46	-38
							Right cerebellum (Crus 1)	<b>0.005</b>	<b>5.58</b>	<b>4.04</b>	<b>34</b>	<b>-76</b>	<b>-32</b>
							Cerebellar vermis	0.002	7.91	4.89	4	-66	-24

Bold indicates main peak of activation within each cluster

<sup>a</sup> Cluster extends into PMD

<sup>b</sup> Cluster extends into S1

magnitude contrast showed extensive activations in areas located primarily in the left primary motor region and bilateral cerebellum. In the cerebellum, a large cluster of activity was observed in the ipsilateral right lobule IV extending into the vermis. In addition, the high force magnitude contrast activated areas in the right temporal and right occipital cortices. No activity was seen in the reversed contrast ([HF/HI, LF/HI]-[HF/LI, LF/LI]).

Regions overlapping in activity during compressions with high instability and high force magnitude

An overlap (yellow, Fig. 3) in activation between the main effects (of force magnitude and instability) was found in the right ipsilateral cerebellum, in lobule VI, and in the left contralateral lobule VI. Apart from this overlap, the clusters of activations for the contrast high instability versus low instability and high force magnitude–low force magnitude were spatially separated. No significant interaction effects were found. This means that the combination of high instability and high force magnitude did not load synergistically (i.e., in a non-additive way) on any region.

## Discussion

The main goal of the present study was to identify brain activity related to the control of two critical functions for manipulation (force magnitude control and instability requirements) of deformable and unstable objects. The novelty lies in that we were able to independently vary the required magnitude of fingertip force and the instability

requirements (i.e., the dynamical control of direction of fingertip force vectors) within the same task, while controlling for other factors common to all conditions. The dynamical control of fingertip force direction, represented by the main effect of high instability, was associated with activity in the bilateral precentral gyri, postcentral gyri/sulci at the level of the intraparietal sulci, and bilaterally in the cerebellum (lobule VI), while fingertip force magnitude (i.e., the main effect of stiffer springs requiring higher forces) was related to unilateral activation of the (contralateral) precentral gyrus and bilateral cerebellum as well as activity in occipital and temporal regions. The bilateral activation is in agreement with previous neuroimaging studies on grip-lift tasks showing increased bilateral activation of premotor areas and primary motor areas with increased demands on somatosensory control and sensory motor processing (Ehrsson et al. 2000, 2001; Gallea et al. 2005).

The present results suggest that force magnitude and stability are controlled by different parts of the grasping network, which has been described in studies on stable objects (Binkofski et al. 1999a, b; Ehrsson et al. 2000, 2001, 2002, 2003; Gallea et al. 2005; Kuhtz-Buschbeck et al. 2001). This network is largely replicated in the conjunction analysis in the present study. Our findings are supported by a previous behavioral study, which demonstrated a unique latent trait during performance of the strength–dexterity paradigm, uncorrelated with grip strength that was suggested to represent the “dexterity component”, that is, the ability to control the direction of the force vectors at the fingertips (Vollmer et al. 2010).

Several grip-lift fMRI studies on stable objects have suggested that the intraparietal sulci and the cerebellum are

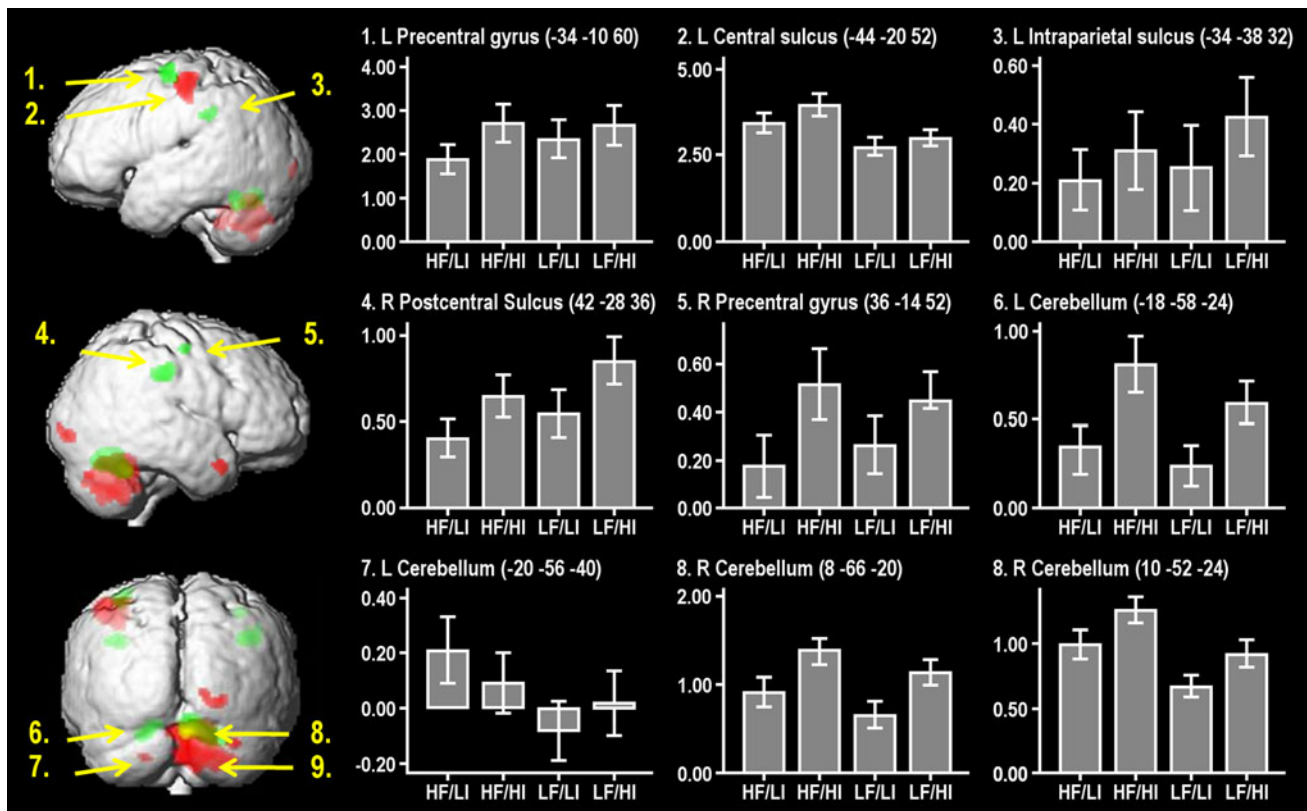


**Fig. 3** Fitted responses of active conditions in peak voxels reported in the main effects analysis (force and instability). Regions active in relation to high–low instability (green), high–low force magnitude (red), and regions that are active for both contrasts (yellow). Values on Y-axis represent mean adjusted BOLD response from local

maxima of motor-related activations during the four conditions, with the mean activity during rest (set to zero) used as baseline. X-axis represents the four conditions, T-bars represent  $\pm 1$  SE of percent signal change induced by each of the individual active conditions. L left, R right

involved in on-line adjustments of movements through implementation of internal models (Bursztyn et al. 2006; Ehrsson et al. 2002; Flanagan et al. 2006; Flanagan and Wing 1997; Jenmalm et al. 2006; Kawato 1999; Kawato et al. 2003; Ohki et al. 2002; Olivier et al. 2007). The process involves the comparison of the actual movement outcome with the predicted movement, and forthcoming adjustments needed to reach the task goal. A common feature of the various grip-lifting tasks is that the performance relies on continuous sensory feedback. The feedback is used to adapt the finger force output; both to correct force magnitude errors (Jenmalm et al. 2006; Johansson and Westling 1988) and, as in the present study, to keep the fingertip force vectors within defined stability limits, set by an internal model of the task performance. The process of controlling the direction of the fingertip forces during manipulation of unstable objects can thus be conceptualized as an internal model of the object and task constraints against which new incoming sensory information is compared. If the force vector approaches the stability limits stipulated by the task constraints, a counteracting adjustment will be executed to adapt the force vector to stay within the limits. Exactly what sensory information is used

to adjust the fingertip forces and update the internal model is not known. However, fast-adapting cutaneous receptors in the fingertips may play a significant role since they can detect small tension in the skin and monitor the balance between the grip force and the lifting force, that is, the direction of the force vector (Johansson and Flanagan 2009).

The neural correlates of the process correcting erroneously programmed grip-lifts were explored in a previous fMRI study (Jenmalm et al. 2006). When the weight of an object was unpredictably changed, activity was found in the ipsilateral inferior parietal cortex (supramarginal gyrus), regardless of whether the weight was lighter or heavier than predicted. The findings thus suggest that the supramarginal cortex is involved in the comparison of the predicted and actual sensory input, while the contralateral primary and somatosensory areas are associated only with a corrective response increasing the grip force, and the ipsilateral cerebellum is associated only with a fast termination of excessive force. Increased activity in the supramarginal cortex was found in the conjunction analysis of the present study supporting the interpretation by Jenmalm et al. that this area is involved in the comparison of predicted and actual sensory information.

The active role of the cerebellum in on-line adjustments has been described during another dynamic grip force task (Milner et al. 2007). In that study, a complex object consisting of a weighted flexible ruler had to be balanced in equilibrium using a precision grip. This was compared with grasping a simple object, that is, a soft foam ball. The ipsilateral cerebellum was strongly activated when balancing the weighted ruler, but not when grasping the foam ball. The interpretation of these findings is complicated by the fact that the two objects differ in numerous properties apart from their demands on dynamic force control. The fact that similar cerebellar areas were activated in the present study, where demands on dynamic force control were systematically varied in the same type of object, while other factors were kept constant, provides strong evidence that these regions are essential for such control. Cerebellar involvement in error correction has also been shown in a recent study on fine motor control by Tanaka et al. (2009), in which participants pressed the right index finger against a force transducer at two different movement rates (0.4 or 0.8 Hz). The left (ipsilateral) cerebellum ( $x = 18$ ,  $y = 52$ ,  $z = 38$ ) showed stronger activation at the slower movement rate, and there was a strong linear relationship between individual errors and activity in the cerebellum at both movement rates. We used a movement rate of 0.5 Hz, that is, close to the slow rate used in the Tanaka study. Our paradigm was not designed to study error correction per se, and the subjects always managed to complete the task. However, the activation of closely the same area in the ipsilateral cerebellum ( $x = 18$ ,  $y = 58$ ,  $z = 24$ ) as in the Tanaka study suggests that there are continuous on-line adjustments and corrections of movements, which are more intense during the high instability condition.

Although a number of brain regions were active in all conditions versus rest (Table 1), it was only in the cerebellum that the main effect analyses revealed activity increases related to both increased force and stability demands. Neurons in this region are known to be involved in finger manipulation and presumably in regulating finger tip forces, possibly in relation to internal models. During the high instability conditions, one would expect an increased activation of these neurons, seen as increased signal in the main effect for stability. In addition, increased force production involves recruitment of additional motor neurons, which might in turn induce activity in a greater number of neurons in hand motor regions of the cerebellum. This in turn should be seen in the main effect for high force vs. low force.

Our results are also compatible with a recent fMRI study investigating brain activity during compression of springs with constant force requirements but varying instability requirements (Mosier et al. 2011). In addition to increased

activity in the bilateral fronto-parieto-cerebellar network during compression of more unstable springs, they noted increased activity in basal ganglia that was not found in the present study. Also in this study, the bilateral fronto-parieto-cerebellar network was engaged during compression of more unstable springs. However, in contrast to these previous findings, we do not detect any activity in the basal ganglia above rest, neither in the conjunction between active conditions nor in the whole-brain main effects analysis. This could reflect a lower signal-to-noise ratio due to the fact that we used a 1.5-T rather than 3-T magnet, and the fact that we used a larger slice thickness and gap in order to cover the whole brain. Alternatively, the basal ganglia may in our study increase their activity in response to both production of precise force amplitudes and directional stability, with little difference in overall level of activity between conditions.

The results of the current study indicate that tasks that mainly require generation and control of fingertip force magnitude (normal to the spring end surface) predominantly engage a different part of the classical grasping network than tasks that also require precise control of fingertip force direction. Increased brain activity associated with the contrast high force–low force magnitude was seen in the contralateral primary motor regions, central sulcus, and bilateral cerebellum. These results are consistent with previous findings regarding the positive correlation between level of force production and activity in M1 (Ehrsson et al. 2000, 2001; Gallea et al. 2005; Kutz-Buschbeck et al. 2001). The activity in M1 was stronger during the compression of the stiffer springs, probably reflecting an increased activation of hand and forearm muscles. The interpretation that M1 is involved in force magnitude control, and less so in the control of the direction of the force vector, is in agreement with Milner et al. (2006, 2007), who reported that M1 was not involved in manipulation dynamics of mechanically unstable objects. This conclusion is further supported by Dafotakis et al. (2008), who showed that inhibiting M1 with TMS did not disrupt reactive adjustments of grip force magnitude during object manipulation.

In conclusion, by varying two fundamental features of dexterous manipulation within the same precision grip task, we were able to identify different areas within the grasping network in which activity co-varied to a different degree with the force magnitude and instability requirements of the task. To our knowledge, this is the first report that discriminates between these two critically different control functions within the same task. Our interpretation is that these areas reflect a context-sensitive system of brain regions that enables dexterous manipulation for different force magnitude and instability requirements.

**Acknowledgments** This work was supported by the Swedish Research Council (5925), Swedish Foundation for Strategic Research, VINNOVA, Foundation Frimurare Barnhuset, Strategic Neuroscience Program at Karolinska Institutet and Knut and Alice Wallenberg, Foundation Stiftelsen Olle Engkvist Byggmästare. BV was funded by a Marie Curie Intra-European Fellowship within the EU FP6 Framework Programme. This work was supported in part by grants (to FVC) NSF 0237258, and NIH HD048566 and AR050520. The authors are thankful to Peter Fransson, Ph.D., for his comments on the initial design of the fMRI paradigm, and to Kristine Mosier, DMD, Ph.D., for her insightful comments and suggestions on the manuscript.

## References

- Ashburner J, Friston K (1997) Multimodal image coregistration and partitioning—a unified framework. *Neuroimage* 6(3):209–217
- Binkofski F, Buccino G, Posse S, Seitz RJ, Rizzolatti G, Freund H (1999a) A fronto-parietal circuit for object manipulation in man: evidence from an fMRI-study. *Eur J Neurosci* 11(9):3276–3286
- Binkofski F, Buccino G, Stephan KM, Rizzolatti G, Seitz RJ, Freund HJ (1999b) A parieto-premotor network for object manipulation: evidence from neuroimaging. *Exp Brain Res* 128(1–2):210–213
- Bursztyn LL, Ganesh G, Imamizu H, Kawato M, Flanagan JR (2006) Neural correlates of internal-model loading. *Curr Biol* 16(24):2440–2445
- Dafotakis M, Sparing R, Eickhoff SB, Fink GR, Nowak DA (2008) On the role of the ventral premotor cortex and anterior intraparietal area for predictive and reactive scaling of grip force. *Brain Res* 1228:73–80
- Duvernoy HM (1999) The human brain: surface, blood supply and three-dimensional sectional anatomy. Springer, Wien
- Ehrsson HH, Fagergren A, Jonsson T, Westling G, Johansson RS, Forssberg H (2000) Cortical activity in precision- versus power-grip tasks: an fMRI study. *J Neurophysiol* 83(1):528–536
- Ehrsson HH, Fagergren E, Forssberg H (2001) Differential fronto-parietal activation depending on force used in a precision grip task: an fMRI study. *J Neurophysiol* 85(6):2613–2623
- Ehrsson HH, Kuhtz-Buschbeck JP, Forssberg H (2002) Brain regions controlling nonsynergistic versus synergistic movement of the digits: a functional magnetic resonance imaging study. *J Neurosci* 22(12):5074–5080
- Ehrsson HH, Fagergren A, Johansson RS, Forssberg H (2003) Evidence for the involvement of the posterior parietal cortex in coordination of fingertip forces for grasp stability in manipulation. *J Neurophysiol* 90(5):2978–2986
- Eickhoff SB, Stephan KE, Mohlberg H, Grefkes C, Fink GR, Amunts K, Zilles K (2005) A new SPM toolbox for combining probabilistic cytoarchitectonic maps and functional imaging data. *Neuroimage* 25(4):1325–1335
- Flanagan JR, Wing AM (1997) The role of internal models in motion planning and control: evidence from grip force adjustments during movements of hand-held loads. *J Neurosci* 17(4):1519–1528
- Flanagan JR, Bowman MC, Johansson RS (2006) Control strategies in object manipulation tasks. *Curr Opin Neurobiol* 16(6):650–659
- Friston KJ, Ashburner J, Frith CD, Poline JB, Heather JD, Frackowiak RSJ (1995) Spatial registration and normalization of images. *Hum Brain Mapp* 2:165–189
- Gallea C, de Graaf JB, Bonnard M, Pailhous J (2005) High level of dexterity: differential contributions of frontal and parietal areas. *Neuroreport* 16(12):1271–1274
- Genovese CR, Lazar NA, Nichols T (2002) Thresholding of statistical maps in functional neuroimaging using the false discovery rate. *Neuroimage* 15(4):870–878
- Jenmalm P, Schmitz C, Forssberg H, Ehrsson HH (2006) Lighter or heavier than predicted: neural correlates of corrective mechanisms during erroneously programmed lifts. *J Neurosci* 26(35):9015–9021
- Johansson RS, Flanagan JR (2009) Coding and use of tactile signals from the fingertips in object manipulation tasks. *Nat Rev Neurosci* 10(5):345–359
- Johansson RS, Westling G (1988) Coordinated isometric muscle commands adequately and erroneously programmed for the weight during lifting task with precision grip. *Exp Brain Res* 71(1):59–71
- Kawato M (1999) Internal models for motor control and trajectory planning. *Curr Opin Neurobiol* 9(6):718–727
- Kawato M, Kuroda T, Imamizu H, Nakano E, Miyauchi S, Yoshioka T (2003) Internal forward models in the cerebellum: fMRI study on grip force and load force coupling. *Prog Brain Res* 142:171–188
- Kuhtz-Buschbeck JP, Ehrsson HH, Forssberg H (2001) Human brain activity in the control of fine static precision grip forces: an fMRI study. *Eur J Neurosci* 14(2):382–390
- Kuhtz-Buschbeck JP, Gilster R, Wolff S, Ulmer S, Siebner H, Jansen O (2008) Brain activity is similar during precision and power gripping with light force: an fMRI study. *Neuroimage* 40(4):1469–1481
- Kwong KK, Belliveau JW, Chesler DA, Goldberg IE, Weisskoff RM, Poncelet BP, Kennedy DN, Hoppel BE, Cohen MS, Turner R et al (1992) Dynamic magnetic resonance imaging of human brain activity during primary sensory stimulation. *Proc Natl Acad Sci U S A* 89(12):5675–5679
- Mayka MA, Corcos DM, Leurgans SE, Vaillancourt DE (2006) Three-dimensional locations and boundaries of motor and premotor cortices as defined by functional brain imaging: a meta-analysis. *Neuroimage* 31(4):1453–1474
- Milner TE, Franklin DW, Imamizu H, Kawato M (2006) Central representation of dynamics when manipulating handheld objects. *J Neurophysiol* 95(2):893–901
- Milner TE, Franklin DW, Imamizu H, Kawato M (2007) Central control of grasp: manipulation of objects with complex and simple dynamics. *Neuroimage* 36(2):388–395
- Mosier KM, Lau C, Wang Y, Venkadesan M, Valero-Cuevas FJ (2011) Controlling instabilities in manipulation requires specific cortical-striatal-cerebellar networks. *J Neurophysiol* 105(3):1295–1305
- Nichols T, Brett M, Andersson J, Wager T, Poline JB (2005) Valid conjunction inference with the minimum statistic. *Neuroimage* 25(3):653–660
- Ogawa S, Tank DW, Menon R, Ellermann JM, Kim SG, Merkle H, Ugurbil K (1992) Intrinsic signal changes accompanying sensory stimulation: functional brain mapping with magnetic resonance imaging. *Proc Natl Acad Sci USA* 89(13):5951–5955
- Ohki Y, Edin BB, Johansson RS (2002) Predictions specify reactive control of individual digits in manipulation. *J Neurosci* 22(2):600–610
- Olivier E, Davare M, Andres M, Fadiga L (2007) Precision grasping in humans: from motor control to cognition. *Curr Opin Neurobiol* 17(6):644–648
- Talati A, Valero-Cuevas FJ, Hirsch J (2005) Visual and tactile guidance of dexterous manipulation tasks: an fMRI study. *Percept Mot Skills* 101(1):317–334
- Tanaka Y, Fujimura N, Tsuji T, Maruishi M, Muranaka H, Kasai T (2009) Functional interactions between the cerebellum and the premotor cortex for error correction during the slow rate force production task: an fMRI study. *Exp Brain Res* 193(1):143–150
- Valero-Cuevas FJ, Smaby N, Venkadesan M, Peterson M, Wright T (2003) The strength-dexterity test as a measure of dynamic pinch performance. *J Biomech* 36(2):265–270
- Vollmer B, Holmstrom L, Forsman L, Krumlinde-Sundholm L, Valero-Cuevas FJ, Forssberg H, Ullen F (2010) Evidence of validity in a new method for measurement of dexterity in children and adolescents. *Dev Med Child Neurol* 52(10):948–954